Empirical stream thermal sensitivities cluster on the landscape according to geology and climate

Lillian M. McGill[1], E. Ashley Steel[2], Aimee H. Fullerton[3]

[1]Center for Quantitative Sciences, University of Washington, Seattle, WA 98105, USA, ORCID ID: 0000-0003-2722-2917
[2]School of Aquatic and Fishery Sciences, University of Washington, Seattle, WA 98105, USA, ORCID ID: 0000-0001-5091-276X
[3]Northwest Fisheries Science Center, National Oceanic and Atmospheric Administration, 2725 Montlake Blvd. East, Seattle, WA 98112, USA, ORCID 0000-0002-5581-3434

Correspondence to: Lillian M. McGill (lmcgill@uw.edu)

Abstract

Climate change is modifying river temperature regimes across the world. To apply management interventions in an effective and efficient fashion, it is critical to both understand the underlying processes causing stream warming and identify the streams most and least sensitive to environmental change. Empirical stream thermal sensitivity, defined as the change in water temperature with a single degree change in air temperature, is a useful tool to characterize historical stream temperature conditions and to predict how streams might respond to future climate warming. We measured air and stream temperature across the Snoqualmie and Wenatchee basins, Washington during hydrologic years 2015-2021. We used ordinary least squares regression to calculate seasonal summary metrics of thermal sensitivity and time-varying coefficient models to derive continuous estimates of thermal sensitivity for each site. We then applied classification approaches to determine unique thermal sensitivity regimes and, further, to establish a link between environmental covariates and thermal sensitivity regime. We found a diversity of thermal sensitivity responses across our basins that differed in both timing and magnitude of sensitivity. We also found that covariates describing underlying geology and snowmelt were the most important in differentiating clusters. Our findings and our approach can be used to inform strategies for river basin restoration and conservation in the context of climate change, such as identifying climate insensitive areas of the basin that should be preserved and protected.

1 Introduction

Globally, river temperature regimes are shifting in response to a changing climate. As water temperature is a critical component of aquatic ecosystems, these changes will alter an essential element of the habitat of many lotic organisms (Daufresne and Boët 2007). To apply management interventions in an effective and efficient fashion, it is critical to both understand the underlying processes causing stream warming (Arismendi et al. 2014, Steel et al. 2017) and identify the streams most and least sensitive to environmental change (Parkinson et al. 2016, Pyne and Poff 2017, Jackson et al. 2018). Measures of empirical stream thermal sensitivity, defined as the change in water temperature

with a single degree change in air temperature, or the slope of the statistical relationship between air temperature and water temperature, address both concerns.

Thermal sensitivities reflect the combined influence of both spatially and temporally varying meteorological and hydrological factors, and a large body of literature examines hypothesized climate, landscape, and hydrogeologic drivers of thermal sensitivity (Table 1A). Variation in solar radiation is often the most important driver of both air and river temperature, and as a result, air and river temperatures are typically correlated (Johnson 2003, Leach et al. 2023). Landscape features such as riparian canopy cover and topographic shading associated with steep watersheds can reduce exposure to solar radiation, suppressing stream temperatures (Webb and Zhang 1997). Stream temperature is also influenced by discharge through changes to thermal inertia and residence time (Meier et al. 2003) and runoff composition where snowmelt, surface runoff, or groundwater inflow entering the stream have different temperature signatures than the stream itself (Webb and Zhang 1997, Mohseni and Stefan 1999, Cadbury et al. 2008). Inputs from water sources such as snowmelt and groundwater upwelling decouple air and water temperatures and result in a decreased thermal sensitivity of water temperature to air temperature (Tague et al. 2007, Mayer 2012, Johnson et al. 2014). As a result, the relationship between air and water temperature can also be a useful diagnostic tool for identifying putative hydrological processes for which empirical measures are often unavailable. Thermal sensitivity has been used in the past to estimate areas of shallow and deep groundwater influence (Snyder et al. 2015, Briggs et al. 2018) and understand the role of snowmelt in modulating river temperature (Lisi et al. 2015, Winfree et al. 2018). Despite conceptual agreement about hypothesized drivers of thermal sensitivity, substantial uncertainty persists regarding the relative importance of these covariates in controlling and predicting thermal sensitivity.

Empirical stream thermal sensitivity has been widely used to characterize historical stream temperature conditions and to predict how streams might respond to future climate warming (Mohseni et al. 2003, Mantua et al. 2010). Generally, larger thermal sensitivities indicate that water temperatures are more likely to track changes in air temperature (Isaak et al. 2016, Mauger et al. 2017, Isaak et al. 2018b). However, there are concerns about using current-day thermal sensitivities to predict future stream temperatures, as it can be difficult to derive insights about river response to perturbations from statistical models that rely on historical relationships that may not extrapolate well to future conditions. For example, past studies have found that using empirical relationships for extrapolating to future climate scenarios without accounting for underlying processes such as snowmelt, groundwater, and annual hysteresis may provide inaccurate predictions of future stream temperatures (Leach and Moore 2019, Steel et al. 2019).

Under changing climatic conditions, the interrelations between air temperature and other processes controlling stream temperature may not remain stable (Arismendi et al. 2014). Additionally, stream networks can exhibit patchy thermal conditions due to spatially heterogeneous landscape attributes such as riparian shading, valley form and aspect, and geology (Bogan et al. 2003, Benyahya et al. 2010). Large-scale models that do not incorporate fine-scale variation in thermal sensitivity may not accurately predict thermal habitat at ecologically relevant scales. Despite these shortcomings, thermal sensitivity remains a commonly used and straightforward tool that allows for comparison between locations within rivers and has the potential to guide management.

There is a need to better understand how thermal sensitivities evolve throughout the year and along river networks and to develop a clearer understanding of the relationships between derived model coefficients and important watershed processes. Furthermore, thermal sensitivity itself can vary across time and space, rendering stationary values insufficient to describe variability in this parameter. A clearer vision of how thermal sensitivities vary would allow natural resource managers to understand what a single snapshot in time or space represents and could provide insight into how river thermal sensitivity may evolve under nonstationary air temperature and precipitation regimes. Groups of streams (clusters) that share similar patterns of thermal sensitivity will likely also share similar risk profiles. Identification of stream clusters could help managers tailor investment in streams according to watershed-specific influences (Mayer 2012). This study aims to answer three questions across two Pacific Northwest river basins: **1)** What is the spatial and temporal distribution of commonly used thermal sensitivity metrics across each basin? **2)** What are the representative thermal sensitivity regimes , how do they cluster on the landscape, and how do these clusters differ from clusters based on air and water temperature individually? and **3)** What are the landscape or climate factors that best predict thermal sensitivity cluster membership? Finally, we consider the statistical functionality of these methods on river networks.

2 Methods

2.1 Study Area

The Snoqualmie River begins as three distinct forks in the Mt. Baker Snoqualmie National Forest and drains a 1,813 km^2 watershed on the west side of the Cascade Range, Washington (Figure 1). The three forks originate in forested public land before converging and flowing through a mix of agricultural, residential, and commercial land use. On one major tributary, the Tolt River, a dam and a large reservoir provide drinking water for the City of Seattle (Figure

S4). The Wenatchee River drains 3,440 km^2 of the eastern Cascades before flowing into the Columbia River (Figure S5). Although land use is similar to the Snoqualmie basin, wherein the headwaters originate in forested public lands before flowing through a mix of agricultural, residential, and commercial land use, forest density is generally lower in the eastern Cascades.

Both the Snoqualmie and Wenatchee basins have a Mediterranean climate with dry summers and wet, mild winters influenced by proximity to the Pacific Ocean. The climate on the east side of the Cascades is drier than that of the west side; the average annual precipitation is 1874 mm (939 mm) and the average annual temperature is 5.7°C (5.3°C) for the western (eastern) Cascades . However, the prevailing westerly winds, which cross the Cascades, create temperature and precipitation gradients that vary widely across the Wenatchee basin. In both basins, precipitation occurs predominately from October to March. The coldest month is typically January, whereas the warmest is July. Rivers have a mixed rain-snow hydrology with substantial winter rain and spring snowmelt, although the Wenatchee basin receives more winter precipitation as snow. Peak flow generally occurs during winter in the Snoqualmie River and spring in the Wenatchee River (Figure 2). Geology differs across the basins. Geology of the Snoqualmie basin is characterized by a deep glacial aquifer in the lowland portion of the watershed, whereas in the alpine area much of the ground surface is directly underlain by bedrock that lacks significant fracture systems (Turney et al. 1995, Bethel 2004). In contrast, the Wenatchee basin's geology consists of both an aquifer within the sedimentary bedrock of the central and lowland areas and an overlying unconsolidated alluvial and outwash aquifer located primarily in river valley bottoms (Montgomery Water Group 2003). The Snoqualmie and Wenatchee basins both have reaches where water temperature exceeds regulatory thresholds established for salmonids that are protected by the U.S. Endangered Species Act (ESA). Both basins support ESA-listed Chinook Salmon (*Oncorhynchus tshawytscha*) and Steelhead Trout (*Oncorhynchus mykiss*) and the Wenatchee basin additionally supports populations of Bull Trout (*Salvelinus confluentus*) and Sockeye Salmon (*Oncorhynchus nerka*).

Water temperature loggers ($N_{Snoqualmie}$=42, $N_{Wenatchee}$=31) were installed throughout the mainstems, on major tributaries and on a selection of minor tributaries for both the Snoqualmie and Wenatchee rivers (Figure 1). Practical limitations forced sites to be publicly accessible, or on private property with landowner permission, and within 1 km of a road. For this study, water temperature was recorded using HOBO TidbiT v2 (UTBI-001) loggers every hour from October 1, 2014 through September 30, 2021 in both basins. We hereafter use North American hydrologic years (1 October – 30 September) instead of calendar years with the year of summer data as the year of reference. Air

temperature data was recorded using HOBO Pendant (UA-002-64) loggers every hour at all water temperature monitoring sites. Air temperature was logged for subset of 11 (6) sites in the Snoqualmie (Wenatchee) basin beginning October 1, 2014, and for all sites beginning October 1, 2016 (October 1, 2018). Air loggers were placed on trees along the stream bank, as close to the stream temperature loggers as possible. The air temperature loggers were secured at approximately breast height on the north side of the trees. Solar shields were fashioned to house both water and air temperature loggers.

2.2 Exploratory analysis of air-water correlation summary metrics

We calculated two summary metrics to characterize the relationship between air temperature and water temperature. For each site, summary metrics were derived from linear regressions between mean daily values of air and water temperature. The slope of this relationship, the thermal sensitivity, indicates the average difference in water temperature when comparing time periods with a one-degree difference in air temperature. For example, a thermal sensitivity of 0.5 would indicate that, based on historical data, when air temperature at a site differs by 1°C, water temperature differs on average by 0.5°C (Leach and Moore 2019). The strength of this relationship (R^2) is an indicator of how well water temperature can be approximated by air temperature and is calculated as the Pearson correlation value between air and water temperature. Summary metrics were calculated separately for each season. Seasons were defined as fall (October, November, December), winter (January, February, March), spring (April, May, June), and summer (July, August, September).

Watersheds for each site were delineated and covariates describing the watersheds were obtained from commonly available geostatistical products (Table 2). Covariates were divided into four broad categories: basin topography (watershed area, mean watershed elevation, average stream slope, and distance upstream), land use (percent watershed forest, riparian forest, and lake area), climate (average temperature, precipitation, and percent precipitation falling as snow), and hydrogeologic (baseflow index, hydraulic conductivity, and soil depth to bedrock). Temperature, precipitation, and percent precipitation as snow were obtained from DAYMET Daily Surface Weather data (Thornton et al. 2020) and all other landscape covariates were obtained from the Stream-Catchment (StreamCat) Database (Hill et al. 2016).

A large body of literature examines landscape-level drivers of air and water temperature correlations within rivers. Therefore, we first summarized hypothesized drivers of thermal sensitivity based on previous literature and their covarying landscape variables within our basins (Table 1A). We then conducted an exploratory analysis of the

relationship between landscape covariates and thermal sensitivity to better understand patterns in our data and set up future hypothesis testing. Due to the correlated nature of our dataset, no formal statistical tests were conducted. We plotted summer thermal sensitivity against hypothesized drivers, including mean watershed elevation (MWE), watershed slope, distance upstream, percent riparian forest cover, and substrate hydraulic conductivity. Loess curves were plotted to aid in data visualization, and correlation coefficients between thermal sensitivity and each landscape covariate were used to quantify the strength of the linear relationship.

We also explored the relationship between spring thermal sensitivity and snowmelt, defined as the change in Snow Water Equivalent (SWE) for a given season and denoted as ΔSWE, and between summer thermal sensitivity and mean air temperature and total precipitation. Climatic variables were obtained from gridded DAYMET data products (Thornton, et al. 2020) and calculated for the upstream catchment of each monitoring station.

2.3 Spatially weighted clustering of thermal sensitivity, water temperature, and air temperature

To identify representative regimes of air-water temperature correlations, we employed a varying-coefficient linear model to obtain continuous, daily estimates of thermal sensitivity. We then defined a spatially weighted dissimilarity matrix for use in clustering, which quantifies the spatial correlation in thermal sensitivity time series while accounting for the directed river network structure. We used this spatially weighted dissimilarity matrix with agglomerative hierarchical clustering to identify groups of sites exhibiting similar patterns in thermal sensitivity over time and compared these clusters to those generated using only water or air temperature. Details of each step are provided in the following sections.

2.3.1 Varying coefficient linear model for air-water relationship

To derive a continuous thermal sensitivity metric, we fit a time-varying coefficient model (TVCM) to air and water temperature data. The TVCM is an effective tool for exploring dynamic features of the sensitivity of water temperature with changes in air temperature and uses a parametric linear model but with time-varying coefficients (Li et al. 2014, 2016). For a given site, we described the varying coefficient model for the air–water temperature relationship as:

$$y_t = \beta_{0,t} + x_t\beta_{1,t} + \epsilon_t, t = 1, \dots, T \quad (1)$$

Where $\beta_{0,t}$ and $\beta_{1,t}$are varying intercept and slope coefficients. To estimate the time-varying coefficients, we adopted an ordinary least squares kernel regression with the Nadaraya–Watson estimator, where we fit a set of weighted local regressions with an optimally chosen window size defined by the bandwidth, b, and the weights given by the kernel

function (Hoover 1998, Casas and Fernandez-Casal 2019). The kernel and its bandwidth control the level of smoothing by adjusting the weight that the neighbouring time points have on estimates at ***t***. The bandwidth was set to 0.2 a priori to ensure consistency across time series. We used the Gaussian kernel that is of the form $k(x) = \frac{1}{2}\pi\, e^{-\frac{x^2}{2}}$. The varying intercept term represents the mean water temperature at time *t* and the varying slope term represents the local sensitivity of water temperature to changes in air temperature at time *t*. We used the R package tvReg (Casas and Fernandez-Casal 2021) for implementing the model.

We filtered resultant time series for site-years with > 218 days (60% of the year) and gaps of ≤ 7 days, yielding 250 site-years from 74 sites across both the Snoqualmie and Wenatchee basins. To capture the typical range and timing of thermal sensitivity at each site, we created a single representative time series of thermal sensitivity at each site by calculating the mean daily thermal sensitivity for each day of the year across all years of filtered data. We use this average annual time series for subsequent clustering analyses. To ensure that using an average annual time series of thermal sensitivity was an appropriate choice given the structure of our data, we conducted a supplementary analysis to assess cluster sensitivity to interannual variability (Appendix A). Measured air and water temperature and modelled thermal sensitivities can be visualized at the following link: https://lmcgill.shinyapps.io/TimeVarying_AWC/.

2.3.2 Estimating a spatially weighted dissimilarity matrix

To quantify spatial correlation while accounting for the directed river network structure, we developed a dissimilarity measure for time series of thermal sensitivity, water temperature, and air temperature that incorporated spatial correlation between sites (Haggarty et al. 2015). The general form of the proposed dissimilarity measure between sites *x* and *y* can be written as:

$$d_{xy}^{c} = d_{xy}\widehat{cov}(h_s) \quad (2)$$

where $d_{xy}^{c}$is the spatially weighted dissimilarity matrix, $d_{xy}$is the Canberra distance (Lance and Williams 1967), and $\widehat{cov}(h_s)$ is a valid stream distance-based covariance matrix.

To estimate $\widehat{cov}(h_s)$, we used the tail-down model that was introduced by Ver Hoef and Peterson (2010). Due to the complex structure of the tail-down model, it is necessary to model spatial correlation on a river network with a covariogram. We first estimated the covariance between time series at each site using a classic formula from Cressie (1993), which states that the estimated covariance between sites *x* and *y* is given by

$$\widehat{cov}(x,y) = \sum_{t=1}^{T} \frac{\{x_t - \bar{x}\}\{y_t - \bar{y}\}}{T} \quad (3)$$

where x_t and y_t are the values of the variable (thermal sensitivity, water temperature, or air temperature) at sites *x* and *y* at time *t* and *T* is the total number of discrete times. This results in a single value which summarizes the covariance between the time series at the two sites over the period of interest. We then plotted these point summaries of the covariance between pairs of curves against lags (measured as stream distance) to obtain an empirical stream distance-based covariogram. We fit an exponential covariance function to this empirical covariogram and evaluated the model at relevant distances to obtain an estimated stream distance-based covariance matrix $\widehat{cov}(h_s)$. We used this new covariance matrix to weight the Canberra distance matrix as shown in Equation 2. The final spatially weighted dissimilarity matrix, d_{xy}^c, was then used in clustering analyses.

2.3.3 Agglomerative hierarchical clustering

We used agglomerative hierarchical clustering (AHC) to identify groups of sites where the patterns in thermal sensitivity, water temperature, and air temperature were similar over time using the hclust function in R (R Core Team 2020). AHC is a common clustering method (Olden et al. 2012, Maheu et al. 2016, Savoy et al. 2019, Isaak et al. 2020) where each time series starts in its own cluster, and the hierarchy is built by repeatedly merging pairs of similar clusters separated by the shortest distance (i.e., measured as the similarity between individual times series) until all points are contained in a single cluster. To decide which clusters are merged in every iteration, AHC uses a dissimilarly metric (d_{xy}^c, derived in Equation 2) and a linkage criterion. We used Ward's minimum variance linkage method for clustering, where the distance between two clusters is computed as the increase in the sum of squared differences after combining two clusters into a single cluster. The shortest of these links (minimum increase in the sum of squared differences) that remains at any step causes the fusion of the two clusters whose elements are involved.

A difficulty associated with cluster analysis is determining the most appropriate number of clusters given the data because no a priori optimal number of clusters exists. Clusters resulting from alternative choices can be evaluated through internal cluster validity indices (CVI); there are a variety of CVIs, most of which combine within cluster cohesion (intra-cluster variance) or between cluster separation (inter-cluster variance) to compute a quality measure. There is no universally best CVI (Arbelaitz et al. 2013), therefore we calculated a suite of five CVIs, including the Silhouette, Gap, Davies–Bouldin, Calinski–Harabasz, and generalized Dunn indices, using the NbClust R package

(Charrad et al. 2014). A final number of clusters was determined by a majority rules approach based on the optimal number of clusters suggested by each index (Table S2).

To determine whether clusters assignment were stable, or preserved under a perturbed dataset similar to the original and therefore likely reflective of real differences, we conducted a bootstrapping approach where sites were sampled with replacement and then AHC was performed on the resampled data using the fpc R package (Hennig 2020). For each bootstrapped cluster, we assessed the similarity between each new cluster and the most similar original cluster with the Jaccard index. The Jaccard coefficient ranges from 0 to 1. Clusters with a coefficient larger than 0.75 were considered stable, clusters with a coefficient between 0.5 and 0.75 indicate that the cluster is measuring a pattern in the data but exact site assignment may be doubtful, and clusters with a mean Jaccard coefficient of less than 0.5 were considered unstable and may not reflect a true pattern in the data (Maheu et al. 2016, Savoy et al. 2019). We repeated the bootstrapping procedure 10,000 times; the mean Jaccard coefficient for each cluster is reported in Table 4.

2.3.4 Identification of environmental drivers in thermal sensitivity

We used classification and regression trees (CART; Breiman et al. 1984) to investigate the relative importance of hydrogeologic, climatic, landscape, and basin topography attributes for predicting each site's membership to a thermal sensitivity cluster. CART is typically used to attempt to predict membership to clusters using environmental attributes, and it allows the modelling of nonlinear relationships among mixed variable types and facilitates the examination of intercorrelated variables in the final model (De'ath and Fabricius 2000, Olden et al. 2008). We took an exploratory approach to this analysis due to our relatively small sample size ($N_{Snoqualmie}$ = 42, $N_{Wenatchee}$ = 31), which limited our ability to conduct statistical tests. Therefore, we calculated variable relative importance, defined as the sum of squared improvements at all splits determined by the predictor. These values are scaled to sum to 100 (rounded). To ensure no single site unduly impacted CART results (Krzywinski and Altman 2017), we conducted a supplementary leave-one-out-cross-validation analysis to ensure relative importance estimates were stable across different permutations of the data (Figure S7). We used the R package rpart (Therneau and Atkinson 2019) for implementing the CART model. Covariates examined are described in Table 2.

3 Results

3.1 General patterns in temperature, precipitation, and thermal sensitivity

This analysis included data from seven hydrologic years, each with differing temperature and precipitation patterns. Generally, the years spanned by our dataset were warmer than the historical average (1901-2000), with wetter than average winter and fall months and drier spring and summer months (Figure S1). For the western (eastern) Cascades, all years (2015-2021) have average annual temperatures higher than the long-term average of 8.6 °C (3 °C), although individual seasons were slightly cooler than average. The year 2015 stood out as a year with an exceptionally warm winter, low snowpack, and dry spring. Temperature and precipitation patterns in the western and eastern Cascades were generally similar, however, precipitation anomalies were typically smaller in the eastern Cascades due to the overall lower precipitation in this region (Figure 2; Figure S1).

Summary metrics describing air-water temperature relationships exhibited substantial variation across time (season and year) and space. Across all season-year combinations, thermal sensitivities ranged from 0.05 to 0.97 (mean = 0.54) in the Snoqualmie basin and from 0.06 to 0.74 (mean = 0.42) in the Wenatchee basin (Table 3). Seasonal distributions of thermal sensitivities differed. For example, fall thermal sensitivities were relatively homogeneous, with 90% of values falling between 0.47 and 0.70, whereas spring and summer thermal sensitivities exhibited a broader range of values, with 90% of values falling between 0.30 and 0.84 in spring and 0.25 and 0.78 in summer. Air temperature was generally a good predictor of water temperature, as evidenced by R^2 values that ranged from 0.20 to 0.99 (mean = 0.88) in the Snoqualmie basin and from 0.08 to 0.98 (mean = 0.85) in the Wenatchee basin (Table 3).

Overall, weak and inconsistent patterns emerge in summer between thermal sensitivity and landscape and climate variables (Figure 3; Table 1B). For climate variables, only ΔSWE appeared to have a linear relationship with thermal sensitivity (Figure 3). The relationship between ΔSWE and thermal sensitivity was negative and non-linear, displaying a wedge-shaped pattern wherein large snowmelt events did not reduce thermal sensitivities below 0.25 (Figure 3). For landscape variables, correlation coefficients were overall small ($|\rho| < 0.3$), indicating weak to non-existent linear relationships between landscape covariates and observed thermal sensitivity (Table 1B). A weakly negative relationship between thermal sensitivity and distance upstream was observed for both basins. Percent riparian forests and thermal sensitivity showed no relationship for either basin. The relationship between hydraulic conductivity and thermal sensitivity was weakly positive and parabolic in the Snoqualmie basin.

3.2 Patterns of clustering for water temperatures, air temperatures, and thermal sensitivities

Time-varying thermal sensitivities displayed periods of both high and low values within a season, which was not necessarily represented when looking only at seasonal summary metrics (Figure 4 and Figure 5). Thermal sensitivity varied alongside water and air temperature within the Snoqualmie and Wenatchee basins. Generally, thermal sensitivity rose sharply in late spring, was highest in late summer, declined slowly throughout the fall, and remained depressed through winter and early spring.

Spatially weighted AHC yielded four clusters for thermal sensitivity, with a cluster validity index (CVI) range of 2-4, and two clusters each for air (CVI range of 2-5) and water (CVI range of 2-4) temperature in the Snoqualmie basin, and five clusters for thermal sensitivity (CVI range 2-5) and two clusters each for air (CVI range of 2-3) and water (CVI range of 2-5) temperature in the Wenatchee basin (Figure 4; Figure 5; Table S2). For both basins, clusters of air and water temperature correspond closely with elevational gradients (Figure S4; Figure S5). Higher elevation sites exhibited generally lower magnitudes but similar patterns in air and water temperatures (Table 4). For example, within both basins seasonal water temperatures were synchronized, with the cluster minimum and maximum water temperatures occurring within a day of each other (Table 4). In the Snoqualmie basin, air temperature clusters were stable, with a mean Jaccard index of 0.91 for high elevation sites (Cluster 2, n=11 sites) and 0.73 for low elevation sites (Cluster 1, n=31 sites). Water temperature clusters were slightly less stable, with a mean Jaccard index of 0.65 for high elevation sites (Cluster 2, n=17 sites) and 0.89 for low elevation sites (Cluster 1, n=25 sites). Air and water temperature clusters in the Wenatchee basin were more stable than the Snoqualmie clusters. In the Wenatchee basin, air temperature clusters had a mean Jaccard index of 0.85 for high elevation sites (Cluster 2, n=25 sites) and 0.95 for low elevation sites (Cluster 1, n=6 sites), and water temperature clusters had a mean Jaccard index of 0. 86 for high elevation sites (Cluster 2, n=23 sites) and 0.73 for low elevation sites (Cluster 1, n=8 sites).

Clustering patterns for thermal sensitivity were more complex and less stable than air and water temperature clusters, particularly for the Snoqualmie basin (Figure 4; Figure 5; Table 4). In the Snoqualmie basin, Cluster 1 (n=11 sites) consisted primarily of low elevation tributaries that exhibited stable thermal sensitivities throughout the year, producing a cluster-average range of only 0.15 (Figure 4; Table 4). Cluster 2 was small (n=5 sites), and the distribution of sites within this cluster included three mainstem sites and two high elevation tributaries. Despite the large geographic distances separating sites, this cluster was highly stable with a mean Jaccard index of 0.88. Cluster 2 was characterized by a mean thermal sensitivity of 0.52 and the highest annual variability, with a cluster-average range of

0.45. Cluster 3 was large (n=15 sites) and contained sites located within the upper regions of the Snoqualmie River. Cluster 3 had the lowest mean thermal sensitivity (mean=0.40). Lastly, Cluster 4 (n=11 sites) exhibited the lowest stability of any cluster in the Snoqualmie basin, with a mean Jaccard index of 0.55. Sites in this cluster were mainly situated on the mainstem Snoqualmie and its major tributaries. This cluster was distinguished by the highest mean thermal sensitivity (mean=0.65). In the Wenatchee basin, all five thermal sensitivity clusters were relatively stable. Clusters 1 (n=7 sites), 4 (n=8 sites), and 5 (n=8 sites) demonstrated similar seasonal patterns in thermal sensitivities, with minimum values occurring in late Spring (water days 216, 207, 214) and maximum values occurring in late summer (water days 324, 331, 330). These clusters also showed moderate to high stability (mean Jaccard indices of 0.79, 0.86, and 0.79). Cluster 3 (n=7 sites) exhibited the highest mean thermal sensitivity (mean=0.40) and encompassed primarily low elevation tributaries (Peshastin and Mission Creek; Figure S5). Cluster 2 was unique in that it consisted of a single site (Chumstick Creek) that was nearly always assigned to a unique cluster when included in the bootstrapping procedure. The thermal sensitivity for this site was low (mean=0.29) and virtually flat throughout the year (range = 0.07).

CART analysis indicated that basin topography and hydrogeology were the principal discriminators of thermal sensitivity clusters. The top predictors of cluster membership (i.e., predictors with a greater than 10% increase in mean standard error if removed from the model) were MWE and baseflow index in the Wenatchee basin and watershed slope, MWE, and soil depth in the Snoqualmie basin (Figure 6). Variable importance distributions differed between the Wenatchee and Snoqualmie basins, although in both basins several covariates had similar relative importance values. Covariate distributions also varied across clusters within a basin. In the Snoqualmie basin, Cluster 1 sites were generally below a MWE of 600 meters, whereas Cluster 3 sites were generally mid-sized and high elevation with a low baseflow index. In the Wenatchee basin, Cluster 1, 4, and 5 sites were predominately located at high elevations with steep slopes. Cluster 4 sites exhibited a large proportion of precipitation falling as rain. Sites in Clusters 2 and 3 were generally low elevation sites with a high baseflow index and soil depth.

4 Discussion

Thermal sensitivity varies throughout the year and reflects hydrologic conditions at a given time and place within a watershed; therefore, it should not be conceptualized as a static value. Although summary metrics of thermal sensitivity, such as average values over the summer, can still prove useful and informative, it is essential to

acknowledge the non-stationarity of the relationship between air and water temperature to obtain an accurate understanding of how river temperature responds to changing conditions. We find that underlying geology and climate are important controls on thermal sensitivity across two Pacific Northwest river basins, and thermal sensitivities reflect aspects of river dynamics not redundant with water and air temperature. Overall, this study provides a framework for using thermal sensitivity regimes to improve understanding of factors contributing to stream temperatures and will enable managers to target mitigation and adaptation activities to work best with local conditions within a watershed.

4.1 Patterns of thermal sensitivity clustering

Our analysis of stream air and water temperatures supports the presence of distinct thermal sensitivity regimes, providing an organizing framework for river research and management by identifying sites with similarities across the network. We found that thermal sensitivity regimes reflected non-redundant aspects of river dynamics relative to air and water temperature alone. Air temperature and water temperature clusters closely corresponded to one another and were almost entirely determined by elevation of the temperature loggers, whereas thermal sensitivity clusters showed more variability in annual patterns and were intermixed spatially (Figure 4; Figure 5). Previous studies within the Pacific Northwest found that, generally, colder streams are less sensitive to air temperature fluctuations than warmer streams (Luce et al. 2014, Kelleher et al. 2021). Air and water clustering results are consistent with previous studies that observed broad temporal correspondence of air and river temperature dynamics with differing magnitudes of response (Bower et al. 2004, Chu et al. 2010, Garner et al. 2014, Isaak et al. 2018a). More locally, Isaak et al. (2020) found that across western rivers, much of the information in stream temperature records could be summarized by a relatively limited number of distinct regime components primarily driven by differences in elevation and latitude.

Viewing thermal sensitivity as a continuous parameter adds novel insights to our understanding of river basin functioning. Studies have highlighted the importance of annual shifts in the processes that drive heat budgets as well as the non-stationarity of the resulting statistical relationships (Arismendi et al. 2014, Boyer et al. 2021). Our clustering analysis overcomes these issues by using a varying coefficient model that treats thermal sensitivity as a continuous function through time, rather than a series of discrete summary metrics, and allows clustering based on the entirety of average annual patterns. The observed complexity in thermal sensitivity response hints at the diversity of physical processes controlling stream temperature response and the large, clear shifts in thermal sensitivity magnitude across the year calls into question the common practice of summarizing a river's sensitivity as a static value. The ability to directly observe shifts in the air-water temperature relationships also opens the possibility of using thermal sensitivity

as a diagnostic tool to examine gradual changes in the importance of drivers of water temperature, such as dynamic changes in riparian shading or snowmelt.

4.2 Climate controls on thermal sensitivity

Seasonal variability of thermal sensitivity metrics was evident for our basins. Within both the Snoqualmie and Wenatchee basins, winter thermal sensitivities were low and varied strongly with MWE (Figure 1). Observed low thermal sensitivities in winter were likely due to the non-linear relationship between air and stream temperature at cold temperatures when air temperatures can dip below the water temperature-freezing limit (Mohseni et al. 1998, 1999). Air temperature covaries strongly with elevation in Pacific Northwest basins, and sites that are high in the watershed will experience a greater number of sub-freezing days, and therefore greater decoupling between air and water temperatures. Fall thermal sensitivities were relatively homogeneous whereas spring and summer thermal sensitivities exhibited a broader range of values. We expect thermal sensitivities to be similar during periods of heavy precipitation, when water sources with thermal characteristics distinct from air temperature, such as groundwater and snowmelt, contribute relatively less flow. The greater variability of responses in spring and summer indicates that the relative magnitude of energy exchange processes controlling river temperatures are more diverse than in fall or winter (Hrachowitz et al. 2010).

Snowmelt likely contributed to observed differences in thermal sensitivity across sites in spring and early summer. For summary metrics, the relationship between snowmelt and spring thermal sensitivity formed a wedge-shaped pattern, wherein sites with limited snowmelt displayed both high and low thermal sensitivity, but sites with extensive snowmelt always display low thermal sensitivity (Figure 3). For the clustering analysis, although the proportion of precipitation falling as snow showed limited variable importance, MWE and slope covaried closely with snow accumulation and were among the most important predictors of cluster membership, perhaps masking a statistical signal of snowfall (Figure 6). In both the Snoqualmie and Wenatchee basins, clusters with higher elevation, steeper slope, and greater snowmelt within the catchment had thermal regimes that were less sensitive to changes in air temperature during spring and early summer. Importantly, snowmelt buffering, the process wherein snowmelt-influenced streams have lower thermal sensitivity due to a direct input of cold water and a corresponding increase in flow rates and water depths (van Vliet et al. 2011, Siegel et al. 2022), diminishes throughout the summer. By late summer, high elevation, snowmelt influenced sites were often more sensitive to air temperatures than their low elevation counterparts (Figure 4; Figure 5). Sites within Cluster 4 in the Wenatchee basin were an exception to this

pattern and maintained summer thermal sensitivities that were substantially depressed relative to adjacent locations (e.g., Clusters 1 and 5). This is likely due to snowmelt inputs within these catchments, and points to the importance of high elevation, late-summer snowpack melt as a significant source of summer baseflow and control on water temperatures during the months of greatest heating within these watersheds.

Numerous studies have examined the buffering impact of snowmelt on water temperature due to advective flux from cooler meltwater entering the river. Studies in Alaskan rivers found a linear, negative relationship between summer thermal sensitivity and snowmelt (Lisi et al. 2015, Cline et al. 2020) and a recent study in the Snoqualmie basin found that snowmelt can reduce basin-wide peak summer temperatures, particularly at high elevation tributaries, and the thermal impacts of melt water can persist through the summer (Yan et al. 2021). Our results suggest that snowpack offers substantial buffering to changes in air temperature across mountain river basins, but that the largest impacts are localized across space and time. Climate change is expected to shift snowmelt earlier and reduce snow water resources (Barnett et al. 2005, Musselman et al. 2021). The loss of snow may result in warming in snow-influenced systems and the subsequent homogenization of thermal conditions across basins (Winfree et al. 2018). Homogenization of thermal conditions likely leads to important changes in ecological functions and ecosystem services supported by lost thermal heterogeneity, such as a loss of cold-water patches for Pacific salmon (Brennan et al. 2019).

4.3 Hydrogeologic controls on thermal sensitivity

Hydrogeologic characteristics shaped the relationship between air and water temperatures across the Wenatchee and Snoqualmie basins. The inclusion of baseflow index, hydraulic conductivity, and soil depth in determining cluster membership (Figure 6) implies the importance, and detectability, of groundwater as a key mediator of thermal sensitivity regimes in Pacific Northwest basins. Clusters with high baseflow index, hydraulic conductivity, and soil depth values generally had lower summer and less variable thermal sensitivities (Figure 4; Figure 5; Figure 6), implying greater groundwater influence (Kelleher et al. 2012). Interestingly, despite the clear importance of hydrogeologic metrics in the clustering analysis, results from summary metric exploratory analysis were mixed and, in the Snoqualmie basin, did not align with expectations of a negative relationship between thermal sensitivity and groundwater influence (Table 1B). Although it is possible to infer broad patterns in surface-groundwater connectivity using datasets of interpolated geologic properties (i.e., hydraulic conductivity, soil depth) or water source (i.e., baseflow index), individual hydrogeologic metrics often have substantial uncertainty, do not covary perfectly, and

may be particularly unconstrained for mountain headwater streams (Wolock et al. 2004, Patton et al. 2018, Briggs et al. 2022). Additionally, the influence of these processes can be localized and variable across space (Johnson et al. 2017) and substantially impacted by human modification. The ability to use thermal sensitivity as an empirical measure of groundwater influence, therefore, shows great promise for understanding catchment processes and informing management and restoration actions at ecologically relevant scales (Snyder et al. 2015). Although our approach moves us closer to a mechanistic understanding of the relationship between thermal sensitivity and groundwater, mixed results from our analyses emphasize the need for additional targeted studies.

An investigation of the underlying geology across the Snoqualmie and Wenatchee basins supports our conclusion that low thermal sensitivities are indicative of groundwater inputs. The lowland portion of the Snoqualmie watershed contains a deep, permeable, productive glacial aquifer that is presumed to be the source of summer baseflow to much of the river (Bethel 2004, McGill et al. 2021, Turney et al. 1995). Glacial and interglacial deposits in the valley contain several geohydrologic units with differing aquifer potential (Bethel 2004); however, most deposits can form small but useable aquifers that could be helping to sustain baseflow in summer months (Turney et al. 1995, Soulsby et al. 2004, Blumstock et al. 2015). Soil depth, hydraulic conductivity, and baseflow index were correspondingly high in streams from Clusters 1 and 4 that overlay the lower portion of the watershed (Figure 6). Thermal sensitivities reflected this pattern, wherein generally sites draining low elevation tributaries (Cluster 1) had relatively constant thermal sensitivities throughout the year (Figure 4). Conversely, the upper portion of the Snoqualmie basin is covered by thin soil over impermeable bedrock lacking extensive fracture networks, meaning that rain and snowmelt are not retained in the mountains but are rapidly transmitted to the stream system (Debose and Klungland 1964, Nelson 1971, Goldin 1973, 1992). Sites with catchments predominantly within this upland area tended to belong to Clusters 2 and 3 and displayed high summer thermal sensitivities, perhaps indicating limited groundwater influence.

In the Wenatchee basin, two major aquifers exist: an aquifer within the sedimentary bedrock of the central and lowland areas and an overlying unconsolidated alluvial and outwash aquifer located primarily in river valley bottoms across the basin (Montgomery Water Group 2003). The bedrock aquifer consists of sandstones and shales, which tend to have moderately low permeability. Folding and faulting have caused the shale to break up or fracture and groundwater moves preferentially within these zones of higher secondary permeability. The alluvial and outwash aquifers, on the other hand, exhibit relatively high permeability where groundwater can move easily and are considered

the primary groundwater source (Wildrick 1979, Montgomery Water Group 2003). Cluster 2 in the Wenatchee basin, consisting of a single site located at the mouth of Chumstick Creek (Figure S5), stands out for having a unique, nearly flat thermal sensitivity compared to patterns at other sites (Figure 5). Covariate distributions for the clustering results showed that Chumstick Creek has a relatively high hydraulic conductivity and baseflow index (Figure 6; Figure S8). A transition from low to high permeability glacial material occurs near the mouth of Chumstick Creek (Montgomery Water Group 2003), and it is possible that substantial groundwater discharge occurs near this discontinuity (Neff et al. 2019). Similarly, sites within Cluster 3 showed low variability in thermal sensitivity and had high soil depth and baseflow index values. Streams within this cluster are situated on top of predominantly sandstone bedrock (Frizzell 1979, Gendaszek et al. 2014).

Overall, the importance of groundwater is consistent with previous studies, which find that thermal sensitivity decreased with increasing groundwater contribution (O'Driscoll and DeWalle 2006, Chang and Psaris 2013, Beaufort et al. 2020, Georges et al. 2021). The degree to which groundwater decouples trends in stream and air temperature depends on stream volume, the rate of groundwater inflow, and the depth of groundwater source. Although not examined in this study, aquifer source and groundwater depth likely influence thermal sensitivity estimates, with runoff sourced from deep groundwater being less variable and less sensitive in comparison to groundwater sourced from shallow sub-surface flows (Tague et al. 2007, Johnson et al. 2021, Hare et al. 2021). Shallow groundwater temperatures are already responding to climate change (Menberg et al. 2014). As warming continues, the summer cooling capacity of groundwater may be reduced, limiting the availability of cold-water refugia patches sourced by groundwater (Brewer 2013, Briggs et al. 2013).

4.4 Landscape controls on thermal sensitivity

Variable relationships between thermal sensitivities and landscape covariates highlight complexities in stream thermal regimes. For example, mean channel slope was an important predictor of cluster membership for both the Snoqualmie and Wenatchee basins, but showed a weak-to-non-existent relationship with summer thermal sensitivity summary metrics. Steeper channel slopes and greater stream velocities limit warming in streams by decreasing the time for equilibration with local heating conditions (Donato 2002, Webb et al. 2008, Isaak et al. 2012) and topographic shading associated with steep watersheds can suppresses stream temperature by reducing exposure to solar radiation (Webb and Zhang 1997). In the Wenatchee basin, the Cluster 3 site, Chumstick Creek, drains a steep canyon. This may contribute to observed low, stable thermal sensitivities throughout the year. Additionally, watershed size and distance

upstream covary closely and displayed relatively consistent relationships with summer thermal sensitivity summary metrics despite ranking moderately in variable importance. We expected thermal sensitivity to increase with river size; groundwater influence should be more visible on smaller streams because the volume of water is small and the travel time of the water from the source is short and not sufficient to equilibrate water temperature with the atmosphere (Mohseni and Stefan 1999, Tague et al. 2007, Beaufort et al. 2016). Reduced sensitivity of headwater streams to air temperature was observed in the Aberdeenshire Dee, Scotland (Hrachowitz et al. 2010), and River Danube, Austria (Webb and Nobilis 2007), and small Pennsylvanian streams were shown to be less sensitive to changes in air temperature than larger streams (Kelleher et al. 2012). However, Hilderbrand et al. (2014) found no relationship between thermal sensitivity and watershed size in Maryland streams.

We expected landscape covariates to be important predictors of thermal sensitivity regimes, however, these covariates were of limited importance and showed no relationship with summary metrics (Table 1B; Figure 6). Several factors may account for this. Inherent covariation in river basins can hinder statistical efforts to identify mechanistic links between landscape gradients and features of aquatic ecosystems (Lucero et al. 2011); land cover characteristics may have a small impact that went undetected due to noisy observations or limited variability within our study region. It is also possible that land cover metrics may not adequately describe the intended process. For example, the relative unimportance of riparian shading may be due in part to our metric of shade, which was limited to riparian forest cover and ignored topographic shading and vegetation height. Lastly, human modifications to the river that are not captured by land cover statistics, such as channelization or the presence of dams and reservoirs, may alter thermal sensitivity and obscure natural gradients. For example, areas of the river that are degraded and subsequently disconnected from their floodplain may have artificially high thermal sensitivities, and the release of water from dams and reservoirs has the potential to either warm or cool downstream temperatures, depending on dynamics of where and how impounded water is released (Ahmad et al. 2021, Cheng et al. 2022). Future research could include covariates sinuosity or variance of thalweg depth to better capture these effects. Untangling exact controls will require additional research.

4.5 Assessment of statistical approach

Collecting data on dynamic stream networks over time has inherent challenges that lead to relatively low sample sizes and missing data as well as complex correlation structures across space and time. Our statistical approach was designed to manage these challenges, enabling exploration of several hypotheses. These data, collected at a relatively

large number of sites in a parallel structure across two basins allow an assessment of how sensitive the statistical approach may be to these constraints.

The time series of both air and water temperature used in this analysis have periods of missing values that span weeks to months. Classical clustering techniques require complete datasets, limiting analyses to time series without gaps. To overcome this issue, we calculated a single representative time series at each site that captures the typical range and timing of thermal sensitivity. Alternative options for dealing with missing values include removing data points that do not cover the target time period or imputing missing values by means of statistical procedures or summary metrics (e.g., Savoy et al. 2019, Beaufort et al. 2020). However, we chose not to use these approaches in our study due to the long and inconsistent periods of missing values across sites. We acknowledge that interannual variability in precipitation and temperature impacts river thermal sensitivity, and average time series calculated from differing years may exhibit differences in shape and timing for reasons outside of inherent characteristics (Appendix A). Future studies could use novel clustering methods capable of dealing with sparse datasets, which would provide more detailed information on clusters generated from time periods with robust values versus data scarcity (Carro-Calvo et al. 2021). Alternatively, recent advances in space-time imputation for river basins may prove a fruitful direction (Li et al. 2017).

Our calculation of time-varying thermal sensitives also necessitated decisions regarding what features of the time series to preserve. Selection of the bandwidth parameter and kernel function for the time varying model will impact estimation of thermal sensitivity and intercept. Generally, with larger bandwidth estimates or averaging periods (e.g., daily, weekly, monthly), intercept estimates increase and thermal sensitivity estimates decrease. Decisions of this nature should be approached carefully and with a clear question in mind. For this study, we were interested in seasonal to annual patterns in thermal sensitivity, and thus chose a bandwidth of 0.2, resulting in a smooth seasonal time series. Previous studies have also used regression splines to estimate the time varying relationship between air and water temperatures (Haggarty et al. 2015). This approach smooths data and can account for missing data but may not preserve small-scale features of interest. We chose to use absolute values of our thermal sensitivity time series, as we cared about differences in mean thermal sensitivity as well as correlated variability. Future work could normalize thermal sensitivity time series first to examine only patterns.

While general patterns could be detected through our analysis, the details were sensitive to exactly which sites were sampled and included in the analysis (Figure S7). In dynamic river systems with high spatial heterogeneity

and inherent difficulties with accessing certain areas of the network, this is always likely to be true. Our approach of averaging across years and clustering across sites appears to manage these realities well and provide general guidance on the river networks sampled. For example, cross validation results for CART modelling suggest that certain variables were consistently identified as more influential for cluster prediction and that results were relatively robust to the inclusion of individual data points (Figure S7). Strengthening the assessment of underlying drivers and controls to provide guidance for unsampled river networks will require that similar data sets are collected across more and more river networks. Data can then be assembled and analysed to provide more general conclusions about geologic and climatic controls of river thermal regimes.

4.6 Implications for management and future directions

Classifying rivers based on thermal sensitivity could be a powerful tool when planning for global change. Our results show that annual patterns in thermal sensitivity are diverse and mediated by underlying geology and climate across two Pacific Northwest river basins. Climate change is decreasing snowpack in the region, resulting in earlier runoff and extended summer baseflow (Elsner et al. 2010, Wu et al. 2012), and may decrease groundwater discharge depending on sources and timing of recharge (Brooks et al. 2012, McGill et al. 2021). For many of our study sites, thermal sensitives were highest in late summer during the hottest, lowest flow portion of the year. Previous studies have found that the impact of fluctuations in discharge generally increases during dry, warm periods, when rivers have a lower thermal capacity and are more sensitive to atmospheric warming (van Vliet et al. 2013). High thermal sensitivity in late summer and in high elevation streams, which are typically thought to be climate refuges, is therefore troubling for the conservation of native coldwater species such as Pacific salmon (Mantua et al. 2010; Isaak et al. 2016). Climate change will likely decrease juvenile rearing and spawning habitat quantity and quality, although it is important to note that streams with high thermal sensitivity may still provide adequate habitat in select portions of the year if stress-related thresholds are not exceeded (Armstrong et al. 2021).

Examining thermal sensitivity regimes improves understanding of factors contributing to stream temperatures and may enable managers to target mitigation and adaptation activities to work best with local conditions, thus maximizing benefits given limited resources. For example, given the importance of subsurface geology within the Wenatchee and Snoqualmie basins, targeted actions to restore floodplain functions that recharge aquifers through actions such as placing engineered logjams or reintroducing beavers could be prioritized (Abbe and Brooks 2013, Pollock et al. 2014, Jordan and Fairfax 2022). Additionally, identification of particularly insensitive portions of the

river could help to better constrain areas where coldwater patches exist that may be used as refuges for coldwater fish (Snyder et al. 2020). This process-based approach will be particularly important as non-stationary relationships caused by climate change make it unreliable to use past regressions built under historical climate conditions (Boyer et al. 2021). Furthermore, as longer, more spatially extensive air and water temperature time series become available (Isaak et al. 2017), we can begin to ask questions about 1) the spatial extent of different thermal sensitivity regimes, 2) how interannual variability shifts with climate conditions and geographic context, and 3) detect changes in the external drivers of thermal sensitivities. Such insights will improve our understanding of river ecosystems while offering a suite of new tools for monitoring the impact of management decisions and climate change.

Acknowledgements

We thank Amy Marsha, Roxana Rautu, Akida Ferguson, Shannon Claeson and the many volunteers for help collecting air and water temperature data, and Gordon Holtgrieve, Mark Scheuerell, and Christopher Jordan for suggestions that improved the manuscript. This material is based upon work supported by the National Science Foundation Graduate Research Fellowship under Grant No. DGE-1762114. Any opinion, findings, and conclusions or recommendations expressed in this material are those of the authors and do not necessarily reflect the views of the National Science Foundation.

Author Contributions and Data Availability

All authors conceptualized the study and retrieved the data. LMM analyzed the data and prepared the manuscript with the assistance of EAS and AHF. The data that supports the findings of this study are available at https://github.com/lmcgill/AirWaterCorr/tree/master/data and can be visualized at https://lmcgill.shinyapps.io/TimeVarying_AWC/. The authors have no competing interests to declare.

References

Abbe, T., and A. Brooks. 2013. Geomorphic, Engineering, and Ecological Considerations when Using Wood in River Restoration. Pages 419–451 *in* A. Simon, S. J. Bennett, and J. M. Castro, editors. Geophysical Monograph Series. American Geophysical Union, Washington, D. C.

Ahmad, S. K., F. Hossain, G. W. Holtgrieve, T. Pavelsky, and S. Galelli. 2021. Predicting the Likely Thermal Impact of Current and Future Dams Around the World. Earth's Future 9.

Arbelaitz, O., I. Gurrutxaga, J. Muguerza, J. M. Pérez, and I. Perona. 2013. An extensive comparative study of cluster validity indices. Pattern Recognition 46:243–256.

Arismendi, I., M. Safeeq, J. B. Dunham, and S. L. Johnson. 2014. Can air temperature be used to project influences of climate change on stream temperature? Environmental Research Letters 9:084015.

Armstrong, J. B., A. H. Fullerton, C. E. Jordan, J. L. Ebersole, J. R. Bellmore, I. Arismendi, B. E. Penaluna, and G. H. Reeves. 2021. The importance of warm habitat to the growth regime of cold-water fishes. Nature Climate Change 11:354–361.

Barnett, T. P., J. C. Adam, and D. P. Lettenmaier. 2005. Potential impacts of a warming climate on water availability in snow-dominated regions. Nature 438:303–309.

Beaufort, A., F. Moatar, F. Curie, A. Ducharne, V. Bustillo, and D. Thiéry. 2016. River Temperature Modelling by Strahler Order at the Regional Scale in the Loire River Basin, France: River Temperature Modelling by Strahler Order. River Research and Applications 32:597–609.

Beaufort, A., F. Moatar, E. Sauquet, P. Loicq, and D. M. Hannah. 2020. Influence of landscape and hydrological factors on stream–air temperature relationships at regional scale. Hydrological Processes 34:583–597.

Benyahya, L., D. Caissie, N. El-Jabi, and M. G. Satish. 2010. Comparison of microclimate vs. remote meteorological data and results applied to a water temperature model (Miramichi River, Canada). Journal of Hydrology 380:247–259.

Bethel, J. 2004. An overview of the geology and geomorphology of the Snoqualmie River watershed. King County Water and Land Resources Division, Snoqualmie Watershed Team.

Blumstock, M., D. Tetzlaff, I. A. Malcolm, G. Nuetzmann, and C. Soulsby. 2015. Baseflow dynamics: Multi-tracer surveys to assess variable groundwater contributions to montane streams under low flows. Journal of Hydrology 527:1021–1033.

603 Bogan, T., O. Mohseni, and H. G. Stefan. 2003. Stream temperature-equilibrium temperature relationship. Water
604 Resources Research 39.
605 Bower, D., D. M. Hannah, and G. R. McGregor. 2004. Techniques for assessing the climatic sensitivity of river flow
606 regimes. Hydrological Processes 18:2515–2543.
607 Boyer, C., A. St-Hilaire, and N. E. Bergeron. 2021. Defining river thermal sensitivity as a function of climate. River
608 Research and Applications 37:1548–1561.
609 Breiman, L., J. H. Friedman, R. A. Olshen, and C. J. Stone. 1984. Classification And Regression Trees. First edition.
610 Routledge.
611 Brennan, S. R., D. E. Schindler, T. J. Cline, T. E. Walsworth, G. Buck, and D. P. Fernandez. 2019. Shifting habitat
612 mosaics and fish production across river basins. Science 364:783–786.
613 Brewer, S. K. 2013. GROUNDWATER INFLUENCES ON THE DISTRIBUTION AND ABUNDANCE OF
614 RIVERINE SMALLMOUTH BASS, *MICROPTERUS DOLOMIEU* , IN PASTURE LANDSCAPES OF
615 THE MIDWESTERN USA. River Research and Applications 29:269–278.
616 Briggs, M. A., P. Goodling, Z. C. Johnson, K. M. Rogers, N. P. Hitt, J. B. Fair, and C. D. Snyder. 2022. Bedrock depth
617 influences spatial patterns of summer baseflow, temperature, and flow disconnection for mountainous
618 headwater streams. preprint, Catchment hydrology/Instruments and observation techniques.
619 Briggs, M. A., Z. C. Johnson, C. D. Snyder, N. P. Hitt, B. L. Kurylyk, L. Lautz, D. J. Irvine, S. T. Hurley, and J. W.
620 Lane. 2018. Inferring watershed hydraulics and cold-water habitat persistence using multi-year air and stream
621 temperature signals. Science of The Total Environment 636:1117–1127.
622 Briggs, M. A., E. B. Voytek, F. D. Day-Lewis, D. O. Rosenberry, and J. W. Lane. 2013. Understanding Water Column
623 and Streambed Thermal Refugia for Endangered Mussels in the Delaware River. Environmental Science &
624 Technology 47:11423–11431.
625 Brooks, J. R., P. J. Wigington, D. L. Phillips, R. Comeleo, and R. Coulombe. 2012. Willamette River Basin surface
626 water isoscape (δ^{18}O and δ^{2}H): temporal changes of source water within the river. Ecosphere 3:art39.
627 Cadbury, S. L., D. M. Hannah, A. M. Milner, C. P. Pearson, and L. E. Brown. 2008. Stream temperature dynamics
628 within a New Zealand glacierized river basin. River Research and Applications 24:68–89.
629 Carro-Calvo, L., F. Jaume-Santero, R. García-Herrera, and S. Salcedo-Sanz. 2021. k-Gaps: a novel technique for
630 clustering incomplete climatological time series. Theoretical and Applied Climatology 143:447–460.

631 Casas, I., and R. Fernandez-Casal. 2019. tvReg: Time-varying Coefficient Linear Regression for Single and Multi-
632 Equations in R. SSRN Electronic Journal.
633 Casas, I., and R. Fernandez-Casal. 2021. tvReg: Time-Varying Coefficients Linear Regression for Single and Multi-
634 Equations.
635 Chang, H., and M. Psaris. 2013. Local landscape predictors of maximum stream temperature and thermal sensitivity
636 in the Columbia River Basin, USA. Science of The Total Environment 461–462:587–600.
637 Charrad, M., N. Ghazzali, V. Boiteau, and A. Niknafs. 2014. NbClust: An R Package for Determining the Relevant
638 Number of Clusters in a Data Set. Journal of Statistical Software 61:1–36.
639 Cheng, Y., B. Nijssen, G. W. Holtgrieve, and J. D. Olden. 2022. Modeling the freshwater ecological response to
640 changes in flow and thermal regimes influenced by reservoir dynamics. Journal of Hydrology 608:127591.
641 Chu, C., N. E. Jones, and L. Allin. 2010. Linking the thermal regimes of streams in the Great Lakes Basin, Ontario,
642 to landscape and climate variables: THERMAL REGIMES IN ONTARIO STREAMS. River Research and
643 Applications 26:221–241.
644 Cline, T. J., D. E. Schindler, T. E. Walsworth, D. W. French, and P. J. Lisi. 2020. Low snowpack reduces thermal
645 response diversity among streams across a landscape. Limnology and Oceanography Letters 5:254–263.
646 Cressie, N. A. C. 1993. Statistics for Spatial Data: Cressie/Statistics. John Wiley & Sons, Inc., Hoboken, NJ, USA.
647 Daufresne, M., and P. Boët. 2007. Climate change impacts on structure and diversity of fish communities in rivers.
648 Global Change Biology 13:2467–2478.
649 De'ath, G., and K. E. Fabricius. 2000. Classification and regression trees: a powerful yet simple technique for
650 ecological data analysis. Ecology 81:3178–3192.
651 Debose, A., and M. W. Klungland. 1964. Soil survey of Snohomish County area. US Department of Agriculture, Soil
652 Conservation Service, Washington, D. C.
653 Donato, M. M. 2002. A statistical model for estimating stream temperatures in the Salmon and Clearwater River
654 basins, Central Idaho. Water Resources Investigations Report, U.S. Geological Survey, Washington, D. C.
655 Elsner, M. M., L. Cuo, N. Voisin, J. S. Deems, A. F. Hamlet, J. A. Vano, K. E. B. Mickelson, S.-Y. Lee, and D. P.
656 Lettenmaier. 2010. Implications of 21st century climate change for the hydrology of Washington State.
657 Climatic Change 102:225–260.

Frizzell, V. A. 1979. Petrology and stratigraphy of Paleogene nonmarine sandstones, Cascade Range, Washington. Open-File Report, U.S. Geological Survey.

Garner, G., D. M. Hannah, J. P. Sadler, and H. G. Orr. 2014. River temperature regimes of England and Wales: spatial patterns, inter-annual variability and climatic sensitivity: RIVER TEMPERATURE REGIMES OF ENGLAND AND WALES. Hydrological Processes 28:5583–5598.

Gendaszek, A. S., D. M. Ely, S. R. Hinkle, S. C. Kahle, and W. B. Welch. 2014. Hydrogeologic framework and groundwater/surface-water interactions of the upper Yakima River Basin, Kittitas County, central Washington. Scientific Investigations Report, U.S. Geological Survey.

Georges, B., A. Michez, H. Piegay, L. Huylenbroeck, P. Lejeune, and Y. Brostaux. 2021. Which environmental factors control extreme thermal events in rivers? A multi-scale approach (Wallonia, Belgium). PeerJ 9:e12494.

Goldin, A. 1973. Soil survey of King County area, Washington. US Department of Agriculture, Soil Conservation Service, Washington, D. C.

Goldin, A. 1992. Soil survey of Whatcom County area, Washington. US Department of Agriculture, Soil Conservation Service, Washington, D. C.

Haggarty, R. A., C. A. Miller, and E. M. Scott. 2015. Spatially weighted functional clustering of river network data. Journal of the Royal Statistical Society: Series C (Applied Statistics) 64:491–506.

Hare, D. K., A. M. Helton, Z. C. Johnson, J. W. Lane, and M. A. Briggs. 2021. Continental-scale analysis of shallow and deep groundwater contributions to streams. Nature Communications 12:1450.

Hennig, C. 2020. fpc: Flexible Procedures for Clustering.

Hilderbrand, R. H., M. T. Kashiwagi, and A. P. Prochaska. 2014. Regional and Local Scale Modeling of Stream Temperatures and Spatio-Temporal Variation in Thermal Sensitivities. Environmental Management 54:14–22.

Hill, R. A., M. H. Weber, S. G. Leibowitz, A. R. Olsen, and D. J. Thornbrugh. 2016. The Stream-Catchment (StreamCat) Dataset: A Database of Watershed Metrics for the Conterminous United States. JAWRA Journal of the American Water Resources Association 52:120–128.

Hoover, D. 1998. Nonparametric smoothing estimates of time-varying coefficient models with longitudinal data. Biometrika 85:809–822.

685 Hrachowitz, M., C. Soulsby, C. Imholt, I. A. Malcolm, and D. Tetzlaff. 2010. Thermal regimes in a large upland
686 salmon river: a simple model to identify the influence of landscape controls and climate change on maximum
687 temperatures. Hydrological Processes 24:3374–3391.
688 Isaak, D. J., C. H. Luce, G. L. Chandler, D. L. Horan, and S. P. Wollrab. 2018a. Principal components of thermal
689 regimes in mountain river networks. Hydrology and Earth System Sciences 22:6225–6240.
690 Isaak, D. J., C. H. Luce, D. L. Horan, G. L. Chandler, S. P. Wollrab, W. B. Dubois, and D. E. Nagel. 2020. Thermal
691 Regimes of Perennial Rivers and Streams in the Western United States. JAWRA Journal of the American
692 Water Resources Association 56:842–867.
693 Isaak, D. J., C. H. Luce, D. L. Horan, G. L. Chandler, S. P. Wollrab, and D. E. Nagel. 2018b. Global Warming of
694 Salmon and Trout Rivers in the Northwestern U.S.: Road to Ruin or Path Through Purgatory? Transactions
695 of the American Fisheries Society 147:566–587.
696 Isaak, D. J., S. J. Wenger, E. E. Peterson, J. M. Ver Hoef, D. E. Nagel, C. H. Luce, S. W. Hostetler, J. B. Dunham, B.
697 B. Roper, S. P. Wollrab, G. L. Chandler, D. L. Horan, and S. Parkes-Payne. 2017. The NorWeST Summer
698 Stream Temperature Model and Scenarios for the Western U.S.: A Crowd-Sourced Database and New
699 Geospatial Tools Foster a User Community and Predict Broad Climate Warming of Rivers and Streams.
700 Water Resources Research 53:9181–9205.
701 Isaak, D. J., S. Wollrab, D. Horan, and G. Chandler. 2012. Climate change effects on stream and river temperatures
702 across the northwest U.S. from 1980–2009 and implications for salmonid fishes. Climatic Change 113:499–
703 524.
704 Isaak, D. J., M. K. Young, C. H. Luce, S. W. Hostetler, S. J. Wenger, E. E. Peterson, J. M. Ver Hoef, M. C. Groce, D.
705 L. Horan, and D. E. Nagel. 2016. Slow climate velocities of mountain streams portend their role as refugia
706 for cold-water biodiversity. Proceedings of the National Academy of Sciences 113:4374–4379.
707 Jackson, F. L., R. J. Fryer, D. M. Hannah, C. P. Millar, and I. A. Malcolm. 2018. A spatio-temporal statistical model
708 of maximum daily river temperatures to inform the management of Scotland's Atlantic salmon rivers under
709 climate change. Science of The Total Environment 612:1543–1558.
710 Johnson, S. L. 2003. Stream temperature: scaling of observations and issues for modelling. Hydrological Processes
711 17:497–499.

712 Johnson, Z. C., B. G. Johnson, M. A. Briggs, C. D. Snyder, N. P. Hitt, and W. D. Devine. 2021. Heed the data gap:
713 Guidelines for using incomplete datasets in annual stream temperature analyses. Ecological Indicators
714 122:107229.
715 Johnson, Z. C., C. D. Snyder, and N. P. Hitt. 2017. Landform features and seasonal precipitation predict shallow
716 groundwater influence on temperature in headwater streams. Water Resources Research 53:5788–5812.
717 Johnson, Z. C., J. J. Warwick, and R. Schumer. 2014. Factors affecting hyporheic and surface transient storage in a
718 western U.S. river. Journal of Hydrology 510:325–339.
719 Jordan, C. E., and E. Fairfax. 2022. Beaver: The North American freshwater climate action plan. WIREs Water 9.
720 Kelleher, C. A., H. E. Golden, and S. A. Archfield. 2021. Monthly river temperature trends across the US confound
721 annual changes. Environmental Research Letters 16:104006.
722 Kelleher, C., T. Wagener, M. Gooseff, B. McGlynn, K. McGuire, and L. Marshall. 2012. Investigating controls on the
723 thermal sensitivity of Pennsylvania streams. Hydrological Processes 26:771–785.
724 Krzywinski, M., and N. Altman. 2017. Classification and regression trees. Nature Methods 14:757–758.
725 Lance, G. N., and W. T. Williams. 1967. A general theory of classificatory sorting strategies: II. Clustering systems.
726 The Computer Journal 10:271–277.
727 Leach, J. A., C. Kelleher, B. L. Kurylyk, R. D. Moore, and B. T. Neilson. 2023. A primer on stream temperature
728 processes. WIREs Water 10:e1643.
729 Leach, J. A., and R. D. Moore. 2019. Empirical Stream Thermal Sensitivities May Underestimate Stream Temperature
730 Response to Climate Warming. Water Resources Research 55:5453–5467.
731 Li, H., X. Deng, C. A. Dolloff, and E. P. Smith. 2016. Bivariate functional data clustering: grouping streams based on
732 a varying coefficient model of the stream water and air temperature relationship. Environmetrics 27:15–26.
733 Li, H., X. Deng, D.-Y. Kim, and E. P. Smith. 2014. Modeling maximum daily temperature using a varying coefficient
734 regression model. Water Resources Research 50:3073–3087.
735 Li, H., X. Deng, and E. Smith. 2017. Missing data imputation for paired stream and air temperature sensor data:
736 Missing Data Imputation for Stream and Air Temperature. Environmetrics 28:e2426.
737 Lisi, P. J., D. E. Schindler, T. J. Cline, M. D. Scheuerell, and P. B. Walsh. 2015. Watershed geomorphology and
738 snowmelt control stream thermal sensitivity to air temperature. Geophysical Research Letters 42:3380–3388.

739 Luce, C., B. Staab, M. Kramer, S. Wenger, D. Isaak, and C. McConnell. 2014. Sensitivity of summer stream
740 temperatures to climate variability in the Pacific Northwest. Water Resources Research 50:3428–3443.
741 Maheu, A., N. L. Poff, and A. St-Hilaire. 2016. A Classification of Stream Water Temperature Regimes in the
742 Conterminous USA: Classification of Stream Temperature Regimes. River Research and Applications
743 32:896–906.
744 Mantua, N., I. Tohver, and A. Hamlet. 2010. Climate change impacts on streamflow extremes and summertime stream
745 temperature and their possible consequences for freshwater salmon habitat in Washington State. Climatic
746 Change 102:187–223.
747 Mauger, S., R. Shaftel, J. C. Leppi, and D. J. Rinella. 2017. Summer temperature regimes in southcentral Alaska
748 streams: watershed drivers of variation and potential implications for Pacific salmon. Canadian Journal of
749 Fisheries and Aquatic Sciences 74:702–715.
750 Mayer, T. D. 2012. Controls of summer stream temperature in the Pacific Northwest. Journal of Hydrology 475:323–
751 335.
752 McGill, L. M., J. R. Brooks, and E. A. Steel. 2021. Spatiotemporal dynamics of water sources in a mountain river
753 basin inferred through $\Delta^{2}H$ and $\Delta^{18}O$ of water. Hydrological Processes 35.
754 Meier, W., C. Bonjour, A. Wüest, and P. Reichert. 2003. Modeling the Effect of Water Diversion on the Temperature
755 of Mountain Streams. Journal of Environmental Engineering 129:755–764.
756 Menberg, K., P. Blum, B. L. Kurylyk, and P. Bayer. 2014. Observed groundwater temperature response to recent
757 climate change. Hydrology and Earth System Sciences 18:4453–4466.
758 Mohseni, O., T. R. Erickson, and H. G. Stefan. 1999. Sensitivity of stream temperatures in the United States to air
759 temperatures projected under a global warming scenario. Water Resources Research 35:3723–3733.
760 Mohseni, O., and H. G. Stefan. 1999. Stream temperature/air temperature relationship: a physical interpretation.
761 Journal of Hydrology 218:128–141.
762 Mohseni, O., H. G. Stefan, and J. G. Eaton. 2003. Global Warming and Potential Changes in Fish Habitat in U.S.
763 Streams. Climatic Change 59:389–409.
764 Mohseni, O., H. G. Stefan, and T. R. Erickson. 1998. A nonlinear regression model for weekly stream temperatures.
765 Water Resources Research 34:2685–2692.
766 Montgomery Water Group. 2003. Wenatchee River Basin Watershed Assessment.

767 Musselman, K. N., N. Addor, J. A. Vano, and N. P. Molotch. 2021. Winter melt trends portend widespread declines
768 in snow water resources. Nature Climate Change 11:418–424.
769 Neff, B. P., D. O. Rosenberry, S. G. Leibowitz, D. M. Mushet, H. E. Golden, M. C. Rains, J. R. Brooks, and C. R.
770 Lane. 2019. A Hydrologic Landscapes Perspective on Groundwater Connectivity of Depressional Wetlands.
771 Water 12:50.
772 Nelson, L. M. 1971. Sediment transport by streams in the Snohomish River basin, Washington: October 1967-
773 June1969.
774 O'Driscoll, M. A., and D. R. DeWalle. 2006. Stream–air temperature relations to classify stream–ground water
775 interactions in a karst setting, central Pennsylvania, USA. Journal of Hydrology 329:140–153.
776 Olden, J. D., M. J. Kennard, and B. J. Pusey. 2012. A framework for hydrologic classification with a review of
777 methodologies and applications in ecohydrology: A FRAMEWORK FOR HYDROLOGIC
778 CLASSIFICATION. Ecohydrology 5:503–518.
779 Olden, J. D., J. J. Lawler, and N. L. Poff. 2008. Machine Learning Methods Without Tears: A Primer for Ecologists.
780 The Quarterly Review of Biology 83:171–193.
781 Parkinson, E. A., E. V. Lea, M. A. Nelitz, J. M. Knudson, and R. D. Moore. 2016. Identifying Temperature Thresholds
782 Associated with Fish Community Changes in British Columbia, Canada, to Support Identification of
783 Temperature Sensitive Streams: STREAM TEMPERATURE AND FISH COMMUNITIES. River Research
784 and Applications 32:330–347.
785 Patton, N. R., K. A. Lohse, S. E. Godsey, B. T. Crosby, and M. S. Seyfried. 2018. Predicting soil thickness on soil
786 mantled hillslopes. Nature Communications 9:3329.
787 Pollock, M. M., T. J. Beechie, J. M. Wheaton, C. E. Jordan, N. Bouwes, N. Weber, and C. Volk. 2014. Using Beaver
788 Dams to Restore Incised Stream Ecosystems. BioScience 64:279–290.
789 Pyne, M. I., and N. L. Poff. 2017. Vulnerability of stream community composition and function to projected thermal
790 warming and hydrologic change across ecoregions in the western United States. Global Change Biology
791 23:77–93.
792 R Core Team. 2020. R: A Language and Environment for Statistical Computing. R Foundation for Statistical
793 Computing, Vienna, Austria.

794 Savoy, P., A. P. Appling, J. B. Heffernan, E. G. Stets, J. S. Read, J. W. Harvey, and E. S. Bernhardt. 2019. Metabolic
795 rhythms in flowing waters: An approach for classifying river productivity regimes. Limnology and
796 Oceanography 64:1835–1851.
797 Siegel, J. E., A. H. Fullerton, and C. E. Jordan. 2022. Accounting for snowpack and time-varying lags in statistical
798 models of stream temperature. Journal of Hydrology X 17:100136.
799 Snyder, C. D., N. P. Hitt, and J. A. Young. 2015. Accounting for groundwater in stream fish thermal habitat responses
800 to climate change. Ecological Applications 25:1397–1419.
801 Snyder, M. N., N. H. Schumaker, J. B. Dunham, M. L. Keefer, P. Leinenbach, A. Brookes, J. Palmer, J. Wu, D.
802 Keenan, and J. L. Ebersole. 2020. Assessing contributions of cold-water refuges to reproductive migration
803 corridor conditions for adult salmon and steelhead trout in the Columbia River, USA. Journal of
804 Ecohydraulics:1–13.
805 Soulsby, C., P. J. Rodgers, J. Petry, D. M. Hannah, I. A. Malcolm, and S. M. Dunn. 2004. Using tracers to upscale
806 flow path understanding in mesoscale mountainous catchments: two examples from Scotland. Journal of
807 Hydrology 291:174–196.
808 Steel, E. A., T. J. Beechie, C. E. Torgersen, and A. H. Fullerton. 2017. Envisioning, Quantifying, and Managing
809 Thermal Regimes on River Networks. BioScience 67:506–522.
810 Steel, E. A., A. Marsha, A. H. Fullerton, J. D. Olden, N. K. Larkin, S.-Y. Lee, and A. Ferguson. 2019. Thermal
811 landscapes in a changing climate: biological implications of water temperature patterns in an extreme year.
812 Canadian Journal of Fisheries and Aquatic Sciences 76:1740–1756.
813 Tague, C., M. Farrell, G. Grant, S. Lewis, and S. Rey. 2007. Hydrogeologic controls on summer stream temperatures
814 in the McKenzie River basin, Oregon. Hydrological Processes 21:3288–3300.
815 Therneau, T., and B. Atkinson. 2019. rpart: Recursive Partitioning and Regression Trees.
816 Thornton, M.M., Shrestha, R., Wei, Y., Thornton, P.E., Kao, S., and Wilson, B.E. 2020. DaymetDaymet: Daily
817 Surface Weather Data on a 1-km Grid for North America, Version 4:0 MB.
818 Turney, G. L., S. C. Kahle, and N. P. Dion. 1995. Geohydrology and ground-water quality of east King County,
819 Washington. Water Resources Investigations Report, Prepared in cooperation with Seattle-King County
820 Department of Health Tacoma, Washington, Washington, D. C.

Ver Hoef, J. M., and E. E. Peterson. 2010. A Moving Average Approach for Spatial Statistical Models of Stream Networks. Journal of the American Statistical Association 105:6–18.

van Vliet, M. T. H., W. H. P. Franssen, J. R. Yearsley, F. Ludwig, I. Haddeland, D. P. Lettenmaier, and P. Kabat. 2013. Global river discharge and water temperature under climate change. Global Environmental Change 23:450–464.

van Vliet, M. T. H., F. Ludwig, J. J. G. Zwolsman, G. P. Weedon, and P. Kabat. 2011. Global river temperatures and sensitivity to atmospheric warming and changes in river flow: SENSITIVITY OF GLOBAL RIVER TEMPERATURES. Water Resources Research 47.

Webb, B. W., D. M. Hannah, R. D. Moore, L. E. Brown, and F. Nobilis. 2008. Recent advances in stream and river temperature research. Hydrological Processes 22:902–918.

Webb, B. W., and F. Nobilis. 2007. Long-term changes in river temperature and the influence of climatic and hydrological factors. Hydrological Sciences Journal 52:74–85.

Webb, B. W., and Y. Zhang. 1997. SPATIAL AND SEASONAL VARIABILITY IN THE COMPONENTS OF THE RIVER HEAT BUDGET. Hydrological Processes 11:79–101.

Wildrick, L. 1979. Ground Water Flow System of the Chumstick Drainage Basin. Page 5. Washington State Department of Ecology, Olympia, WA.

Winfree, M. M., E. Hood, S. L. Stuefer, D. E. Schindler, T. J. Cline, C. D. Arp, and S. Pyare. 2018. Landcover and geomorphology influence streamwater temperature sensitivity in salmon bearing watersheds in Southeast Alaska. Environmental Research Letters 13:064034.

Wolock, D. M., T. C. Winter, and G. McMahon. 2004. Delineation and Evaluation of Hydrologic-Landscape Regions in the United States Using Geographic Information System Tools and Multivariate Statistical Analyses. Environmental Management 34:S71–S88.

Wu, H., J. S. Kimball, M. M. Elsner, N. Mantua, R. F. Adler, and J. Stanford. 2012. Projected climate change impacts on the hydrology and temperature of Pacific Northwest rivers: CLIMATE CHANGE IMPACTS ON STREAMFLOW AND TEMPERATURE. Water Resources Research 48.

Yan, H., N. Sun, A. Fullerton, and M. Baerwalde. 2021. Greater vulnerability of snowmelt-fed river thermal regimes to a warming climate. Environmental Research Letters 16:054006.

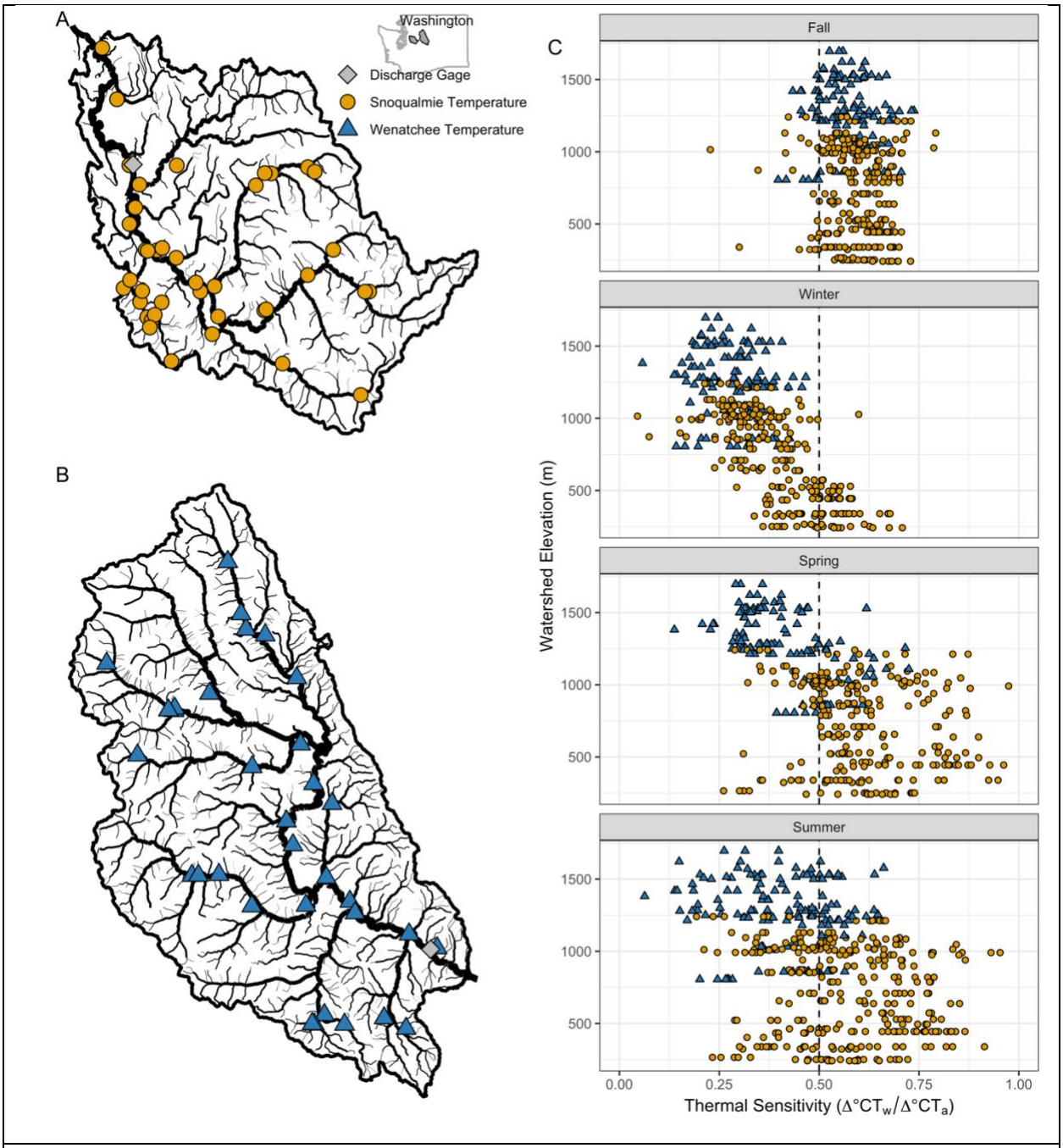

Figure 1. A map of the Snoqualmie (A) and Wenatchee (B) basins water and air temperature monitoring sites and the most downstream USGS gage for each basin. Thermal sensitivity, defined as the change in water temperature with a single degree change in air temperature, versus MWE for each site-year combination (C). The dashed line in Figure 1C is included as a reference.

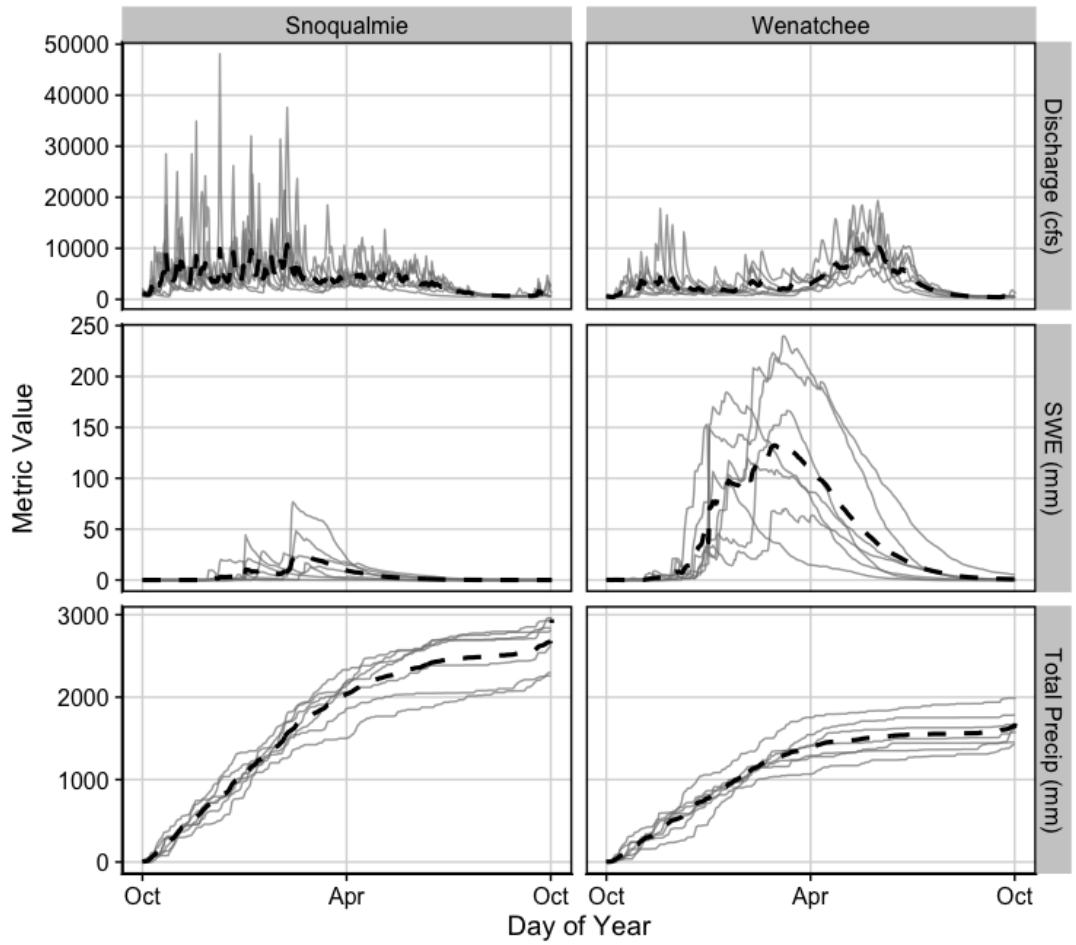

Figure 2. Average annual discharge, SWE, and total precipitation for the outlets of the Snoqualmie and Wenatchee basins across the sampling timeframe (black dashed lines) and interannual variability across the seven water years included in this analysis (gray lines). Discharge gage locations can be found in Figure 1A and 1B, and SWE and precipitation data is from DAYMET Daily Surface Weather data for the upstream watershed of each discharge gage (Thornton et al. 2020).

851

852

853

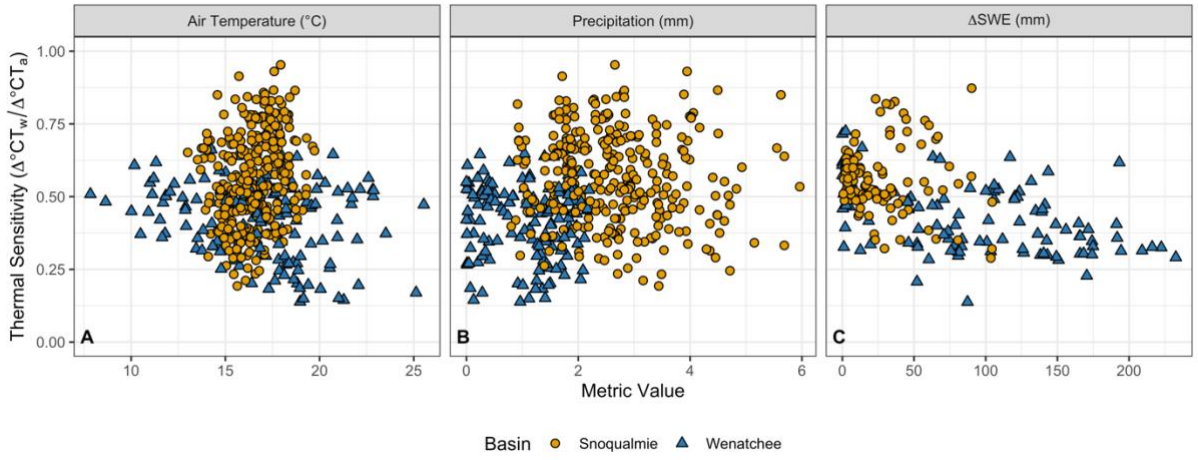

Figure 3. Summer thermal sensitivity values for all site-year combinations in the Snoqualmie and Wenatchee basins versus air temperature (A), and precipitation (B). Spring thermal sensitivity values for all site-year combinations versus total SWE (C) from gridded DAYMET data for each sampling point. Points are colored by basin. Basins that have no snowmelt in a given year are not shown on graph (C).

854

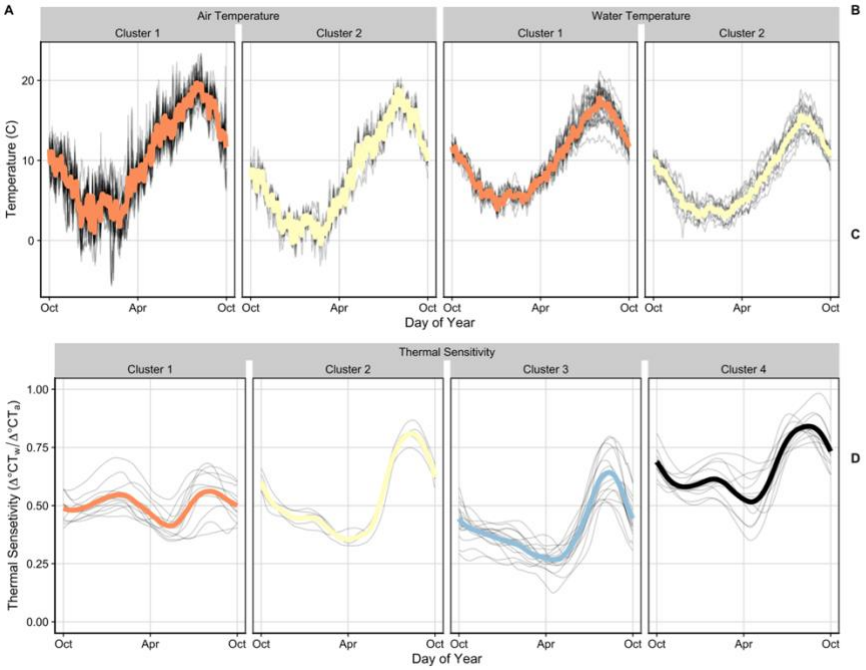

Figure 4. Average time series (A) and spatial clustering results (columns/colors indicate unique clusters) for average annual air temperature (B), water temperature (C), and thermal sensitivity (D) in the Snoqualmie basin. The spatial distribution for colored lines indicates mean average annual values for each cluster, and gray lines denote average annual values for each site within a given cluster.

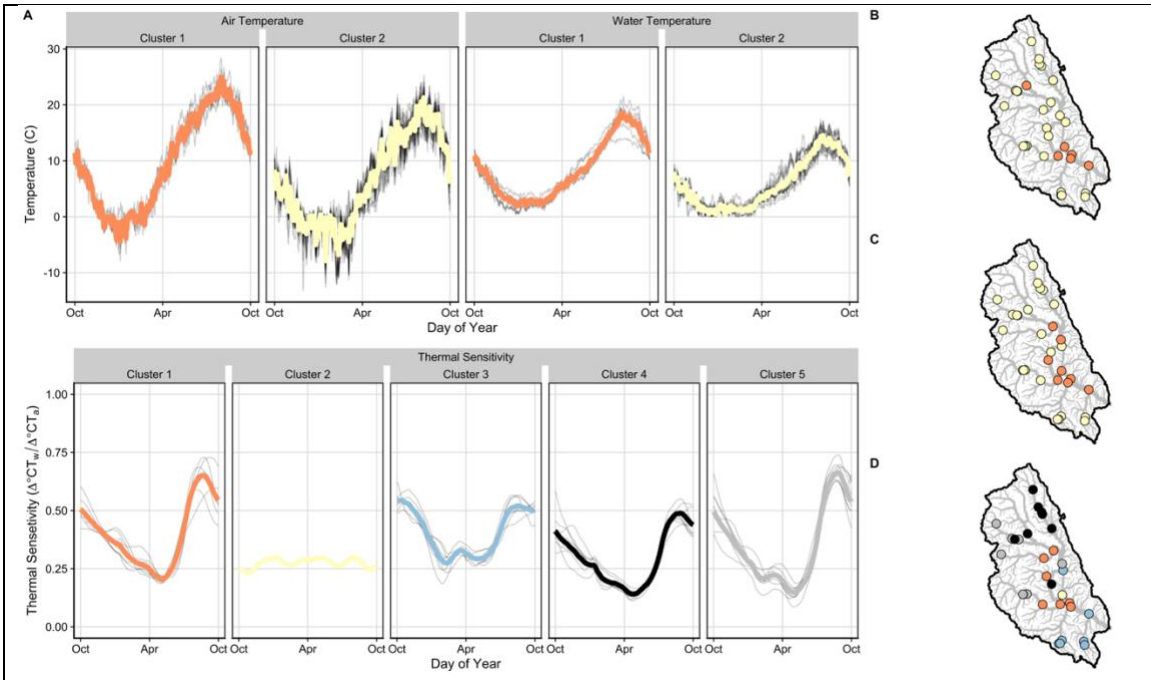

Figure 5. Average time series (A) and spatial clustering results (columns/colors indicate unique clusters) for average annual air temperature (B), water temperature (C), and thermal sensitivity (D) in the Wenatchee basin. The spatial distribution for colored lines indicates mean average annual values for each cluster, and gray lines denote average annual values for each site within a given cluster.

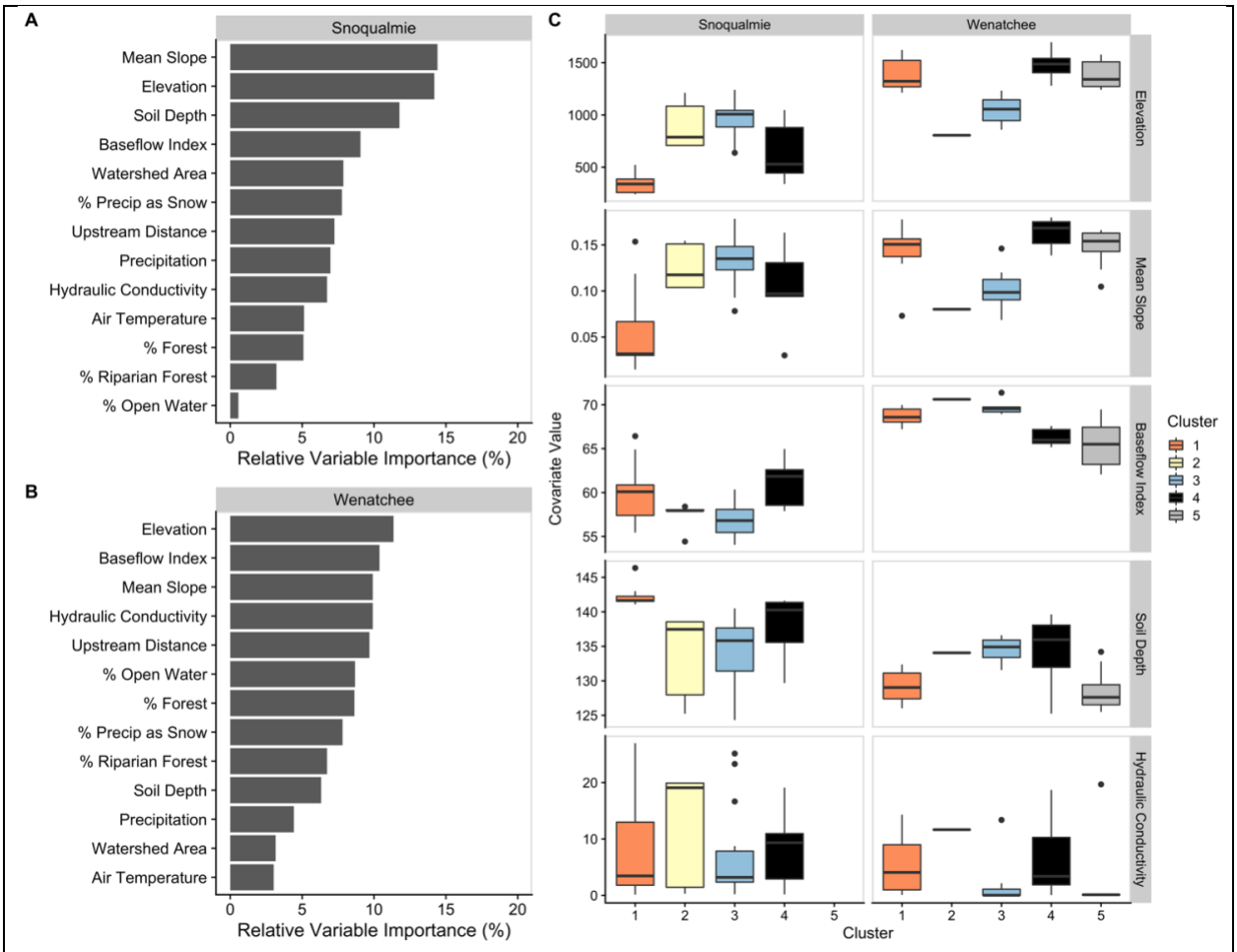

Figure 6. Relative variable importance for all covariates in the Snoqualmie (A) and Wenatchee (B) basins, and the distributions of variables across clusters for the four most important variables (C) in the Snoqualmie basin (Mean Slope, Elevation, Soil Depth, and Baseflow Index) and in the Wenatchee basin (Elevation, Baseflow Index, Mean Slope, and Hydraulic Conductivity). Boxes are grouped and colored by cluster membership. See Figure S8 for plots of the remaining relative variable importances.

Table 1. Hypothesized relationships between landscape covariates and thermal sensitivity based on previous literature (A) and the observed relationship between landscape variables and thermal sensitivities within our study basins in summer (B). Loess curves are shown to aid in visualization and correlation coefficients quantify the strength of the linear relationship. See Figure S6 for a detailed description of how river attributes covary with one another.

A. Hypothesized Drivers			**B. Observed Relationship**
Stream or watershed attribute (covarying variables)	**Theoretical relationship with thermal sensitivity**	**Explanation**	**Observed Relationship in Summer**
Mean watershed slope +elevation +dist upstream – soil depth	Negative	• Increased snowmelt and cooling due to faster velocity water movement and shorter water residence time (Winfree et al. 2018). • Topographic shading associated with steep watersheds suppresses stream temperature by reducing exposure to solar radiation (Webb and Zhang 1997).	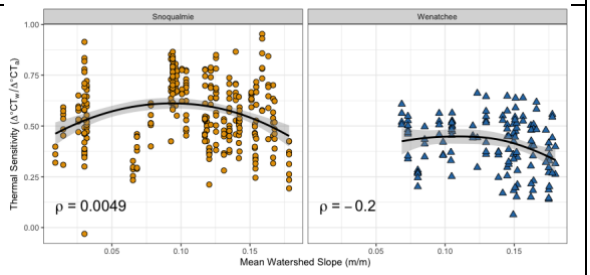
Mean watershed elevation +slope +dist upstream +% lake area – soil depth	Negative	• Higher elevations have higher snowmelt accumulation and greater proportion of snowmelt in spring. • The impact of elevation on spring and early summer stream temperature is diminished in years with low winter snow accumulation.	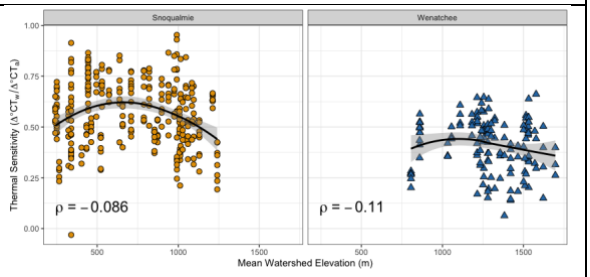
Distance upstream – watershed size +slope +elevation	Negative	• Duration of surface water's exposure to solar radiation and atmospheric energy flux is higher in low gradient watersheds with slower streamflow velocities (Poole and Berman 2001).	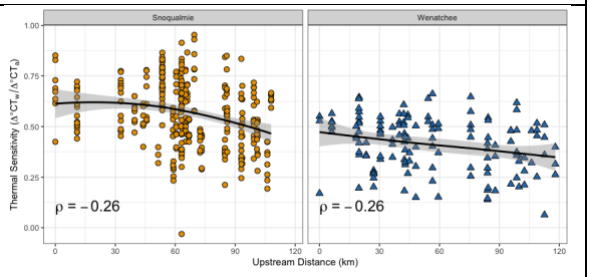
Percent riparian forest cover +% forest cover – watershed size	Negative	• Riparian vegetation provides shading to streams, reducing exposure to solar radiation (Webb and Zhang 1997), particularly during summer base flows. • Forest canopy can influence snow accumulation within a watershed and snowmelt contribution to streams. Low density forests accumulate more snow relative to	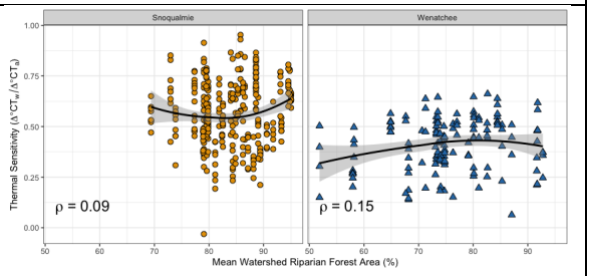

		high density forests (Varhola et al 2010). • Conversion of forested land area can accelerate runoff and reduce infiltration, warming surface flows before they reach stream channels (Naiman et al. 2005; Nelson and Palmer 2007).	
Hydraulic Conductivity +baseflow index	Positive	• Hydraulic conductivity refers to the ability of a geologic material to transmit water and is calculated from mean lithological hydraulic conductivity content in surface or near surface geology. • Relatively high hydraulic conductivity material would be represented by something like unconsolidated alluvial sands and gravels. • High hydraulic conductivity is typically associated with areas of greater groundwater activity and lower, more stable thermal sensitivity values.	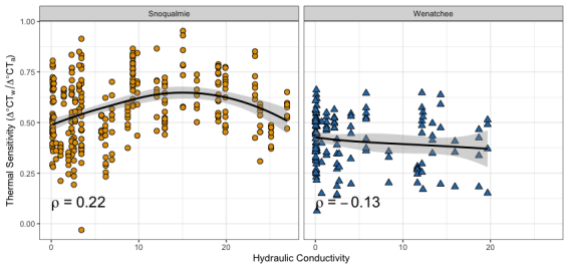

10

Table 2. Physical environmental data and basin characteristics used to predict air-water clusters.

Variable	Category	Units	Data Source
Watershed area	Basin Topography	km^2	Hill et al. 2016
Mean watershed elevation	Basin Topography	m	Hill et al. 2016
Avg. stream slope	Basin Topography	mm^{-1}	Hill et al. 2016
Distance upstream	Basin Topography	km	Hill et al. 2016
% Watershed forest	Land Use	%	Hill et al. 2016; Dewitz et al. 2019
% Riparian forest	Land Use	%	Hill et al. 2016; Dewitz et al. 2019
% Lake area	Land Use	%	Hill et al. 2016; Dewitz et al. 2019
Avg. Temperature	Climate	C	Thornton et al. (2020)
Avg. Precipitation	Climate	mm	Thornton et al. (2020)
Avg. % precip as snow	Climate	%	Thornton et al. (2020)
Baseflow index	Hydrogeologic	%	Hill et al. 2016; Wolock 2003
Hydraulic conductivity	Hydrogeologic	%	Hill et al. 2016; Olson and Hawkins 2014
Soil depth to bedrock	Hydrogeologic	cm	Hill et al. 2016; Carlisle et al. 2009

Table 3. Air water correlation average summary metrics by basin and season. Averages are calculated as the mean value of summary metrics at all sites across each basin and season.

		Thermal Sensitivity			R^2		
		Min	Mean	Max	Min	Mean	Max
Snoqualmie	Fall	0.22	0.59	0.79	0.58	0.92	0.99
	Winter	0.05	0.40	0.71	0.20	0.86	0.96
	Spring	0.26	0.60	0.97	0.67	0.89	0.98
	Summer	0.19	0.56	0.95	0.41	0.85	0.97
Wenatchee	Fall	0.40	0.57	0.74	0.74	0.94	0.98
	Winter	0.05	0.28	0.47	0.44	0.84	0.95
	Spring	0.14	0.42	0.72	0.59	0.88	0.98
	Summer	0.06	0.41	0.66	0.08	0.77	0.96

Table 4. Averaged metrics for all sites within each cluster determined with the spatially weighted agglomerative hierarchical clustering. For timing metrics, days are reported as hydrologic day, where a value of 1 indicates October 1st and a value of 365 indicates September 30th.

Metric	Basin	Cluster	# Sites	Mean	Minimum (timing)	Maximum (timing)	Cluster Stability
Thermal Sensitivity	Snoqualmie	1	11	0.50	0.41 (224)	0.56 (308)	0.68
		2	5	0.52	0.36 (181)	0.81 (315)	0.88
		3	15	0.40	0.27 (201)	0.64 (316)	0.67
		4	11	0.65	0.52 (199)	0.84 (316)	0.55
	Wenatchee	1	7	0.39	0.20 (216)	0.65 (324)	0.79
		2	1	0.27	0.23 (28)	0.30 (101)	0.62
		3	7	0.40	0.27 (131)	0.54 (11)	0.94
		4	8	0.29	0.14 (207)	0.48 (331)	0.86
		5	8	0.35	0.15 (214)	0.66 (330)	0.69
Air	Snoqualmie	1	31	10.2	1.01 (94)	19.7 (305)	0.91
		2	11	8.02	-0.42 (145)	18.9 (304)	0.73
	Wenatchee	1	6	9.68	-4.52 (95)	25.0 (304)	0.95
		2	25	6.48	-7.88 (107)	21.3 (310)	0.85
Water	Snoqualmie	1	25	10.1	3.91 (94)	17.8 (304)	0.65
		2	17	7.99	2.94 (94)	15.6 (304)	0.89
	Wenatchee	1	8	8.39	1.95 (108)	18.5 (310)	0.73
		2	23	5.74	0.37 (107)	14.5 (310)	0.86